Economic Geology
Vol. 85, 1990, pp. 1917–1925

RADICAL SULFUR ISOTOPE ZONATION OF PYRITE ACCOMPANYING BOILING AND EPITHERMAL GOLD DEPOSITION: A SHRIMP STUDY OF THE VALLES CALDERA, NEW MEXICO

MICHAEL A. MCKIBBEN

Department of Earth Sciences and Center for Geothermal Research of the Institute of Geophysics and Planetary Physics, University of California, Riverside, California 92521

AND C. STEWART ELDRIDGE

Geology Department and Research School of Earth Sciences, Australian National University, G.P.O. Box 4, Canberra, A.C.T. 2601, Australia

Introduction

Evidence cited for boiling as a mechanism of precious metals deposition in epithermal systems has traditionally included acidic alteration assemblages and fluid inclusions that have trapped coexisting liquid and vapor (e.g., Berger and Bethke, 1985, and papers therein). Because boiling involves loss of aqueous H_2 and H_2S to the vapor phase, causing an increase in the oxidation state of the residual fluid (Drummond and Ohmoto, 1985), significant fractionation of sulfur isotopes could also be recorded by minerals formed during boiling.

Until now, however, conventional bulk measuring techniques have not provided the data necessary to allow recognition of such significant events in terms of their isotopic systematics. For example, typical bulk $\delta^{34}S$ values for sulfides from many epithermal systems lie close to 0 per mil and give little hint of any isotopic complexity (i.e., Ohmoto and Rye, 1979). An exception is the wide variation in bulk $\delta^{34}S$ value of sulfides associated with the waning stages of the Creede hydrothermal system as reported by Plumlee and Rye (1987). With the advent of advanced in situ ion microprobe techniques capable of examining microscopic variations in the isotopic compositions of individual crystals (Eldridge et al., 1987, 1988a, 1988b, 1989; McKibben and Eldridge, 1989), it is now possible to search for strong isotopic zonation in epithermal sulfides as evidence of precipitation in the zone of boiling. Discovery of radical isotopic zonation in minerals from modern two-phase geothermal systems may allow application of stable isotopic data to the study of epithermal deposits whose origin due to boiling might otherwise be obscured by later processes.

Geologic Setting

The Valles caldera, New Mexico, hosts a modern epithermal system which has been explored by numerous industry and scientific drill holes. Drill hole VC-2a, a 528-m-deep scientific core hole (Goff et al., 1987), penetrated the western caldera ring fracture zone beneath Sulphur Springs, an area of active hot springs and intense acid sulfate alteration (Charles et al., 1986). The borehole penetrated a hydrothermally altered sequence of intracaldera fill, consisting mainly of rhyolitic tuffs and lesser volcaniclastic sediments. Mineralization and hydrothermal alteration found in this drill core have been described by Hulen et al. (1987) and Hulen and Nielsen (1988). In brief, the alteration consists of a shallow highly silicified and sericitized phyllic zone (0–163 m) overlying a deeper moderately altered chlorite-sericite zone (163–528 m). The phyllic zone is now vapor dominated, although textural characteristics of quartz-filled vugs imply the former existence of a liquid-dominated hydrothermal system. Pyrite is the most ubiquitous sulfide mineral throughout the drill core.

One unique aspect of the mineralization is the presence of fluorite and poorly crystalline molybdenite which appear to have been deposited from boiling fluids at temperatures of approximately 200°C in the phyllic zone (Hulen et al., 1987; Sasada and Goff, 1989; Gonzalez, 1989) Hulen and Nielson (1988) and Sasada and Goff (1989) have proposed that this shallow mineralization formed in conjunction with collapse of the southwest caldera wall, less than about 0.5 m.y. ago. The collapse caused a former caldera lake to drain, leading to a drop in hydrostatic head, resulting in boiling, brecciation, and development of the present vapor-dominated shallow system.

The change from liquid to vapor dominance might have lead to sulfide deposition through volatile loss, perhaps according to reactions coupled through the production or consumption of hydrogen ions (e.g., Reed and Spycher, 1985). For example, rapid initial loss of CO_2 and H_2 to the vapor phase may have driven reactions such as:

$$2HCO_3^- + Mo^{+2} + 2H^+ + 2HS^- \rightarrow MoS_2 + H_{2(g)} + 2CO_{2(g)} + 2H_2O \quad (1)$$

and

$$2HCO_3^- + Fe^{+2} + 2H^+ + 2HS^- \rightarrow FeS_2 + H_{2(g)} + 2CO_{2(g)} + 2H_2O. \quad (2)$$

Analytical Materials and Methods

Three VC-2a drill core samples, at depths of 30.5, 57.3, and 129.6 m (100, 188, and 425.3 ft), were

TABLE 1. SHRIMP $\delta^{34}S$ Values of Pyrite Crystals from Drill Core VC-2a

Sample no., analysis no.	Crystal	$^{34}S/^{32}S$ sample	Standard deviation (1σ)	$^{34}S/^{32}S$ Standard	(1σ)	$\delta^{34}S$ sample	Error (2σ)
			30.5-m (100-ft) level				
VC-2A, 1	PY-1 core	0.042732	0.000034	0.043305	0.000017	−2	2
VC-2A, 2	PY-1 rim	0.042756	0.000038	0.043305	0.000017	−1	2
VC-2A, 14	PY-1 core-rim	0.042876	0.000034	0.043359	0.000018	1	2
VC-2A, 3	PY-2 core	0.042824	0.000039	0.043359	0.000018	1	2
VC-2A, 4	PY-2 rim	0.042843	0.000040	0.043359	0.000018	1	2
VC-2A, 5	PY-3 core	0.042807	0.000032	0.043359	0.000018	−1	2
VC-2A, 6	PY-3 rim	0.042735	0.000037	0.043359	0.000018	−3	2
VC-2A, 8	PY-4 core	0.042767	0.000037	0.043359	0.000018	−2	2
VC-2A, 9	PY-5 rim	0.042869	0.000034	0.043359	0.000018	0	2
VC-2A, 10	PY-5 core	0.042784	0.000037	0.043359	0.000018	−2	2
VC-2A, 11	PY-6 core	0.042756	0.000037	0.043359	0.000018	−2	2
VC-2A, 15	PY-6 core	0.042763	0.000034	0.043359	0.000018	−2	2
VC-2A, 12	PY-6 rim	0.042914	0.000034	0.043359	0.000018	1	2
VC-2A, 13	PY-6 core-rim	0.042795	0.000034	0.043359	0.000018	−1	2
VC-2A, 16	PY-7 core	0.042748	0.000036	0.043359	0.000018	−2	2
VC-2A, 17	PY-7 rim	0.042805	0.000035	0.043359	0.000018	−1	2
VC-2A, 18	PY-8 core	0.042804	0.000037	0.043359	0.000018	−1	2
VC-2A, 19	PY-8 rim	0.042775	0.000048	0.043359	0.000018	−2	2
VC-2A, 20	PY-9 core	0.043128	0.000038	0.043689	0.000022	−1	2
VC-2A, 21	PY-10 core	0.043121	0.000040	0.043689	0.000022	−1	2
			57.3-m (188-ft) level				
VC-2A, 72	PY-1 core	0.042823	0.000027	0.043312	0.000018	0	2
VC-2A, 65	PY-2 core	0.042783	0.000024	0.043246	0.000016	1	2
VC-2A, 33	PY-3 core	0.042734	0.000038	0.043195	0.000015	1	2
VC-2A, 11	PY-4 rim	0.042737	0.000041	0.043314	0.000014	−2	2
VC-2A, 64	PY-4 rim	0.042465	0.000025	0.043246	0.000016	−7	2
VC-2A, 15	PY-4 core	0.042721	0.000036	0.043314	0.000014	−2	2
VC-2A, 43	PY-4 core	0.042979	0.000032	0.043436	0.000018	1	2
VC-2A, 63	PY-4 core	0.042621	0.000024	0.043246	0.000016	−3	2
VC-2A, 10	PY-4 rim-core	0.042768	0.000040	0.043314	0.000014	−1	2
VC-2A, 4	PY-5 rim	0.042372	0.000040	0.043314	0.000014	−12	2
VC-2A, 7	PY-5 rim	0.042507	0.000036	0.043314	0.000014	−7	2
VC-2A, 62	PY-5 rim	0.042386	0.000024	0.043246	0.000016	−8	2
VC-2A, 3	PY-5 core	0.042372	0.000040	0.043314	0.000014	−10	2
VC-2A, 54	PY-5 core	0.042507	0.000031	0.043246	0.000016	−6	2
VC-2A, 9	PY-6 rim	0.042514	0.000035	0.043314	0.000014	−7	2
VC-2A, 16	PY-6 rim	0.042252	0.000035	0.043314	0.000014	−13	2
VC-2A, 48	Repeat of analysis 16	0.042536	0.000030	0.043436	0.000018	−7	2
VC-2A, 49	PY-6 rim	0.042631	0.000035	0.043436	0.000018	−7	2
VC-2A, 8	PY-6 core	0.042627	0.000040	0.043314	0.000014	−4	2
VC-2A, 14	PY-6 core	0.042124	0.000038	0.043314	0.000014	−16	2
VC-2A, 53	PY-6 core	0.042532	0.000024	0.043246	0.000016	−5	2
VC-2A, 61	PY-6 core	0.042431	0.000027	0.043246	0.000016	−7	2
VC-2A, 12	PY-7 rim	0.042652	0.000036	0.043314	0.000014	−4	2
VC-2A, 56	PY-7 rim	0.042497	0.000027	0.043246	0.000016	−6	2
VC-2A, 58	PY-7 rim	0.042452	0.000024	0.043246	0.000016	−7	2
VC-2A, 13	PY-7 core	0.042793	0.000041	0.043314	0.000014	0	2
VC-2A, 32	PY-7 core	0.042705	0.000034	0.043195	0.000015	0	2
VC-2A, 55	PY-7 core	0.042730	0.000028	0.043246	0.000016	0	2
VC-2A, 57	PY-7 core	0.042739	0.000027	0.043246	0.000016	0	2
VC-2A, 26	PY-8 rim	0.042508	0.000033	0.043195	0.000015	−4	2
VC-2A, 17	PY-8 core	0.042779	0.000046	0.043314	0.000014	−1	2
VC-2A, 24	PY-8 core	0.042717	0.000033	0.043195	0.000015	1	2
VC-2A, 25	PY-8 core	0.042747	0.000035	0.043195	0.000015	1	2
VC-2A, 27	PY-8 core	0.042819	0.000033	0.043195	0.000015	3	2
VC-2A, 28	PY-9 rim	0.042248	0.000036	0.043195	0.000015	−10	2
VC-2A, 30	PY-9 rim	0.042429	0.000033	0.043195	0.000015	−6	2
VC-2A, 68	PY-9 rim	0.042199	0.000033	0.043312	0.000018	−14	2
VC-2A, 70	PY-9 rim	0.042022	0.000026	0.043312	0.000018	−18	2
VC-2A, 29	PY-9 core	0.042799	0.000036	0.043195	0.000015	3	2
VC-2A, 67	PY-9 core	0.043010	0.000028	0.043312	0.000018	5	2
VC-2A, 31	PY-9 rim-core	0.042335	0.000037	0.043195	0.000015	−8	2
VC-2A, 71	PY-9 rim-core	0.042425	0.000028	0.043312	0.000018	−9	2

TABLE 1. (*Cont.*)

Sample no., analysis no.	Crystal	$^{34}S/^{32}S$ sample	Standard deviation (1σ)	$^{34}S/^{32}S$ Standard	(1σ)	$\delta^{34}S$ sample	Error (2σ)
57.3-m (188-ft) level							
VC-2A, 1	PY-10 rim	0.042588	0.000035	0.043314	0.000014	−6	2
VC-2A, 46	Repeat of analysis 1	0.042797	0.000031	0.043436	0.000018	−3	2
VC-2A, 6	PY-10 rim	0.042450	0.000039	0.043314	0.000018	−8	2
VC-2A, 22	PY-10 rim	0.042648	0.000035	0.043195	0.000015	−1	2
VC-2A, 23	PY-10 rim	0.042648	0.000034	0.043195	0.000015	−1	2
VC-2A, 47	Repeat of analysis 23	0.043016	0.000034	0.043436	0.000018	2	2
VC-2A, 41	PY-10 rim	0.042812	0.000029	0.043436	0.000018	−3	2
VC-2A, 42	PY-10 rim	0.042898	0.000029	0.043436	0.000018	1	2
VC-2A, 51	PY-10 rim	0.042682	0.000025	0.043246	0.000016	1	2
VC-2A, 59	PY-10 rim	0.042400	0.000024	0.043246	0.000016	−8	2
VC-2A, 2	PY-10 core	0.042911	0.000036	0.043314	0.000014	2	2
VC-2A, 45	Repeat of analysis 45	0.042903	0.000034	0.043436	0.000018	−1	2
VC-2A, 5	PY-10 core	0.042979	0.000036	0.043314	0.000014	4	2
VC-2A, 21	PY-10 core	0.043003	0.000035	0.043195	0.000015	7	2
VC-2A, 40	PY-10 core	0.043037	0.000033	0.043436	0.000018	3	2
VC-2A, 52	PY-10 core	0.042928	0.000026	0.043246	0.000016	4	2
VC-2A, 69	Repeat of analysis 52	0.042971	0.000025	0.043312	0.000018	4	2
VC-2A, 60	PY-10 core	0.042625	0.000028	0.043246	0.000016	−3	2
VC-2A, 66	PY-10 core	0.042807	0.000028	0.043246	0.000016	2	2
129.6-m (425.3-ft) level							
VC-2A, 1	PY-1 core	0.043013	0.000031	0.043421	0.000015	2	2
VC-2A, 2	PY-1 rim	0.042869	0.000033	0.043421	0.000015	−1	2
VC-2A, 3	PY-2 core	0.042977	0.000032	0.043421	0.000015	2	2
VC-2A, 4	PY-2 rim	0.042862	0.000031	0.043421	0.000015	−1	2
VC-2A, 5	PY-3 core	0.042918	0.000041	0.043421	0.000015	0	2
VC-2A, 6	PY-3 rim	0.042914	0.000031	0.043421	0.000015	0	2
VC-2A, 7	PY-4 core	0.042808	0.000033	0.043421	0.000015	−3	2
VC-2A, 8	PY-4 rim	0.042836	0.000034	0.043421	0.000015	−2	2
VC-2A, 9	PY-5 core	0.042960	0.000030	0.043421	0.000015	1	2
VC-2A, 10	PY-5 rim	0.043021	0.000030	0.043421	0.000015	3	2
VC-2A, 11	PY-6 core	0.042887	0.000042	0.043421	0.000015	−1	2
VC-2A, 12	PY-6 rim	0.042859	0.000030	0.043421	0.000015	−1	2
VC-2A, 13	PY-7 core	0.042803	0.000034	0.043291	0.000014	0	2
VC-2A, 14	PY-7 rim	0.042665	0.000033	0.043291	0.000014	−3	2
VC-2A, 15	PY-8 rim	0.042795	0.000033	0.043291	0.000014	0	2
VC-2A, 16	PY-8 core	0.042820	0.000034	0.043291	0.000014	1	2
VC-2A, 17	PY-9 rim	0.042808	0.000034	0.043291	0.000014	1	2
VC-2A, 18	PY-10 core	0.042786	0.000032	0.043291	0.000014	0	2
VC-2A, 19	PY-11 core	0.042722	0.000033	0.043291	0.000014	−2	2
VC-2A, 20	PY-12 core	0.042722	0.000032	0.043291	0.000014	−2	2
VC-2A, 21	PY-12 rim	0.042614	0.000033	0.043291	0.000014	−4	2

selected from the phyllic zone on the basis of high Mo contents (Hulen et al., 1987). Examination of polished samples in reflected light revealed no grains of MoS_2 greater than 30 μm across (minimum required for ion microprobe analysis), but the samples do contain disseminated and vein pyrite mineralization within the altered tuffs. The pyrite occurs as individual crystals up to 250 μm in diameter and as clusters up to 500 μm across. Reflected-light examination revealed that many of the disseminated crystals are morphologically zoned with porous impure cores separated from euhedral pure rims by dark growth bands or gaps. Most of the vein pyrite is optically pure and generally euhedral. The pyrite is often accompanied by authigenic quartz.

Approximately ten pyrite crystals were chosen from each of the three samples for in situ sulfur isotope analysis. Analyses were performed using the SHRIMP ion microprobe, at the Australian National University, utilizing techniques, standards, and data treatment as described in Eldridge et al. (1987, 1989). This instrument affords spatial resolution on the order of 30 μm and produces $\delta^{34}S$ values with precisions and accuracies of ± 2 per mil (2σ). In crystals greater than 60 μm across, both core and rim analyses were carried out to determine whether or not any sulfur isotope changes accompanied crystal growth.

Some crystals from the 57.3-m (188-ft) sample were analyzed, repolished, and reanalyzed to check the reproducibility of the data and for the possibility of isotopic zonation with depth in the crystals (i.e., repeated analyses are noted in Table 1). Only two out of the ten areas reanalyzed showed any significant differences: crystals 4 and 9 had $\delta^{34}S$ values slightly lower in the second round compared with the first. These differences may reflect isotopic zoning with depth and/or slight differences in primary beam positioning between analytical sessions.

Aqueous H_2S in the present-day geothermal fluid was collected during flow tests of the VC-2a borehole in 1987. The fluid originated at a depth of 489 m where downhole temperatures were 210°C (Musgrave et al., 1989). H_2S in steam was precipitated as ZnS and converted to Ag_2S in the laboratory for conventional sulfur isotope analysis by gas source mass spectrometry. Conventional determinations of $\delta^{34}S$ for this sample were made by R. O. Rye at the Denver U.S. Geological Survey laboratories.

Aqueous H_2S was also collected from the present-day geothermal fluid in the well VC-2b, located less than 1 km northeast of VC-2a. This well is 1,762 m (5,780 ft) deep and penetrated not only the volcanic sequence but also the underlying Miocene sandstones, Paleozoic sandstones and limestones, and Precambrian quartz monzonite basement (Hulen and Gardiner, 1989). Fluid from depths of 1,695 to 1,762 m ($\simeq$295°C) in the quartz monzonite was sampled during a flow test in June of 1989. H_2S in this fluid was collected and analyzed for its sulfur isotope composition in the same manner as the fluid sample from VC-2a.

Crystals of native sulfur deposited in fumaroles at Sulphur Springs have previously been analyzed for their sulfur isotope composition, yielding $\delta^{34}S$ values of $\simeq$0 per mil (Fr. Goff, pers. commun.)

Analytical Results

Sulfur isotope data for pyrite from this study are presented in Table 1 in per mil relative to the Canyon Diablo troilite standard. Data are grouped according to depth along the core and reported in order from shallowest to deepest levels. The data in Table 1 are also plotted at histograms for individual crystals (Fig. 1) and correlated with textures in Figure 2.

30.5-m level

The ten crystals selected from the 30.5-m (100-ft) level yielded one to three analyses each (Fig. 1A). Contrary to expectations from the obvious morphological zonation, the isotopic data revealed little significant deviation from 0 per mil (Fig. 2A). The crystals examined appear to be isotopically homogeneous as individuals and as a group.

57.3-m level

One to eight sulfur isotopic analyses were performed on each of the ten crystals chosen from the 57.3-m (188-ft) level (Fig. 1B). The sample was repolished in order to repeat several analyses on some crystals. Though some crystals are isotopically homogeneous and indistinguishable in composition from those of the 30.5-m level, this sample exhibited the highest degree of microscopic variation in $\delta^{34}S$ values overall. Pyrite crystals 1, 2, 3, and for the most part, 4 are identical in isotopic composition to those found in the 30.5-m sample. The cores of pyrite crystals 7 and 8 also have $\delta^{34}S$ values close to 0 per mil.

Data from the remaining crystals examined at this level show significant departures from the homogeneous pattern established thus far. There is a strong shift to $\delta^{34}S$ values well below 0 per mil (i.e., to a minimum of −18‰) as well as marked internal isotopic heterogeneity (Fig. 2B and C). Crystals 8, 9, and 10 have also recorded $\delta^{34}S$ values somewhat greater than 0 per mil (Table 1; Figs. 1B and 2C). Despite some complexity within crystal 10, crystals 7 through 10 have a general pattern of isotopically heavy cores with isotopically lighter rims. Isotopically heterogeneous crystals have total ranges in sulfur isotope composition of 8, 11, 7, 8, and 15 per mil (crystals 5, 6, 7, 8, and 10, respectively), with crystal 9 having a maximum range of 22 per mil in a distance of only 75 μm from core to rim (Fig. 2C).

129.6-m level

Twelve crystals were analyzed from this sample, with one to two analytical craters per crystal (Fig. 1C). Like the pyrites from the 30.5-m level, none of the crystals show zonations in $\delta^{34}S$ that exceed the 2 per mil precision of the SHRIMP. Figure 2D shows an example of analytical craters for crystals 1 and 3.

Aqueous H_2S

Aqueous H_2S in VC-2a fluid yielded a conventional $\delta^{34}S$ value of 0.8 per mil, while that from VC-2b fluid yielded a value of 2.5 per mil.

Discussion

The near 0 per mil $\delta^{34}S$ values found for most of the pyrite in this study (30.5-m level; crystals 1 to 3 at the 57.3-m level; 129.6-m level) are indistinguishable from that determined for H_2S in the present-day VC-2a geothermal fluid (0.8‰), suggesting that much of the pyrite precipitated in sulfur isotope equilibrium with similar fluids. Simple cooling or pH increase during wall-rock alteration may have caused most of the pyrite precipitation. The fumarolic sulfur deposits at Sulphur Springs may have obtained H_2S from this fluid as well.

However, dramatic decreases in $\delta^{34}S$ values from core to rim within some of the pyrites from the intermediate depth (crystals 7–10 at the 57.3-m level) indicate that a radical change took place in depositional conditions, fluid chemistry, or source of sulfur.

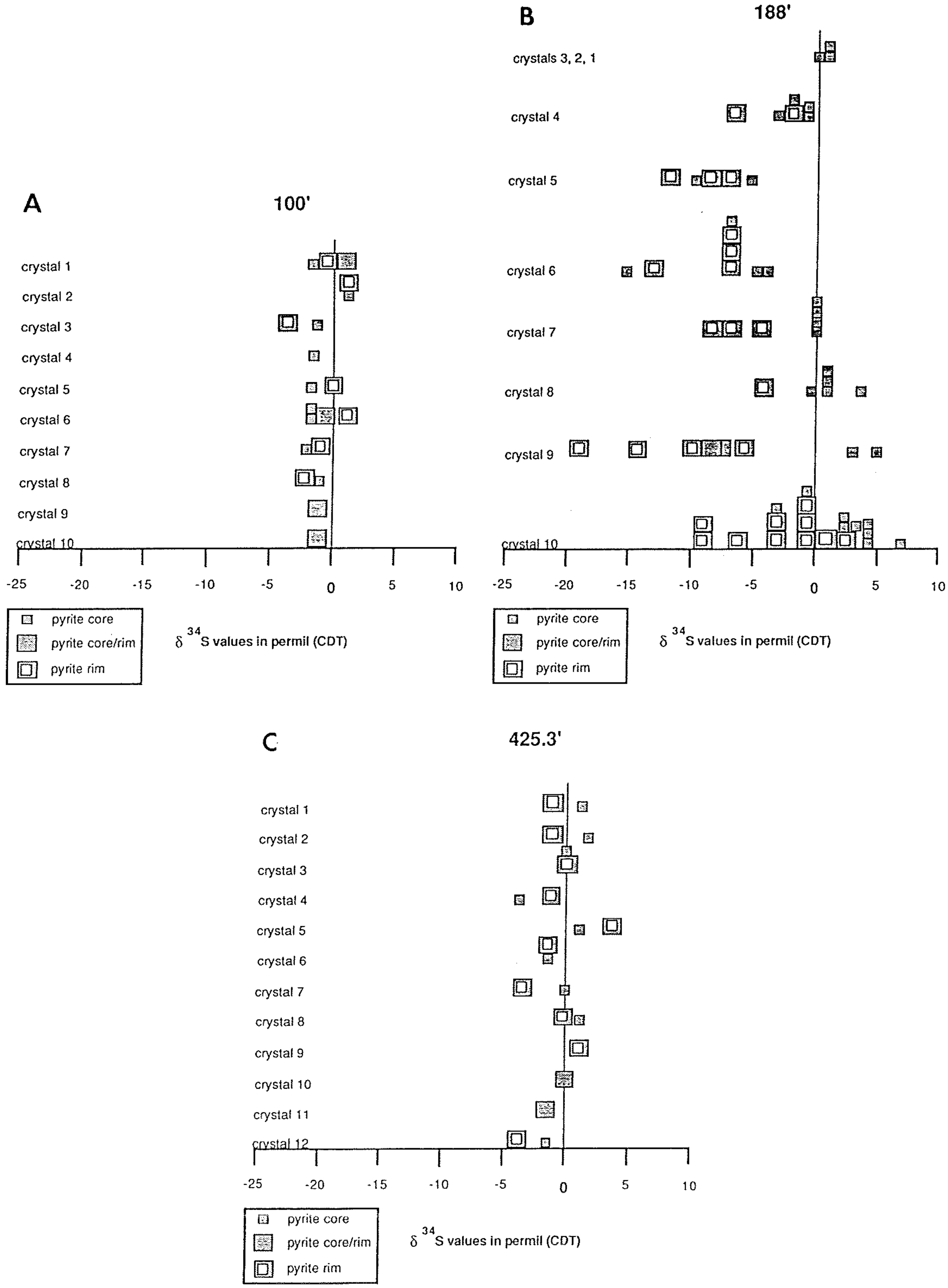

FIG. 1. Histograms of SHRIMP $\delta^{34}S$ values for pyrite crystals in Table 1. A. 30.5-m (100-ft) level. B. 57.3-m (188-ft) level. C. 129.6-m (425.3-ft) level.

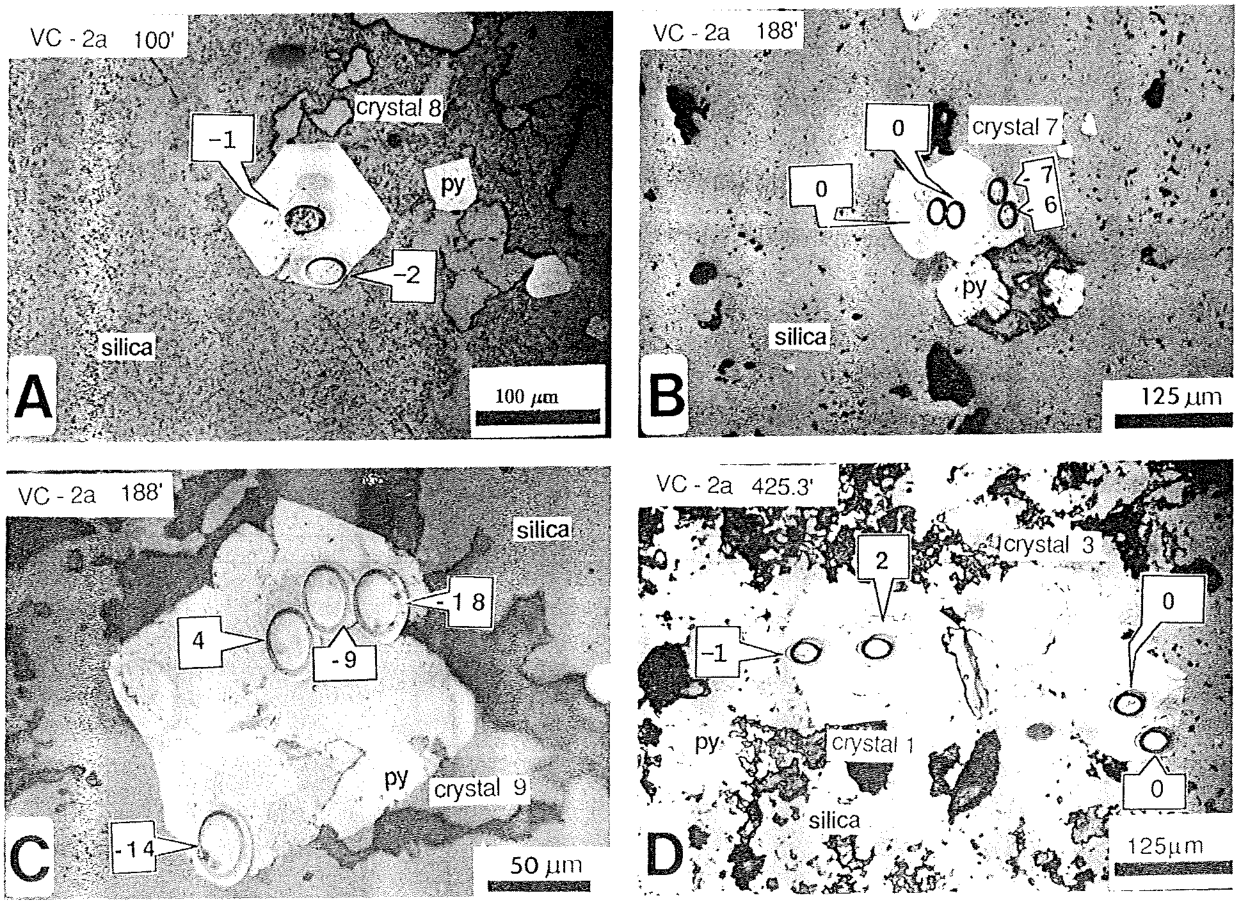

FIG. 2. Microphotographs showing selected SHRIMP analytical craters in pyrite crystals from Table 1. Numbers in arrowed boxes are SHRIMP $\delta^{34}S$ values in per mil. A. 30.5-m (100-ft) level, crystal 8. B. 57.3-m (188-ft) level, crystal 7. C. 57.3-m (188-ft) level, crystal 9. D. 129.6-m (425.3-ft) level, crystals 1 and 3.

The latter can probably be ruled out. The $\delta^{34}S$ value of H_2S in deeper VC-2b fluids originating from the basement rocks (2.5‰) indicates that deeper source rocks in the Valles caldera do not contain fluids with sulfur isotope compositions that are radically different

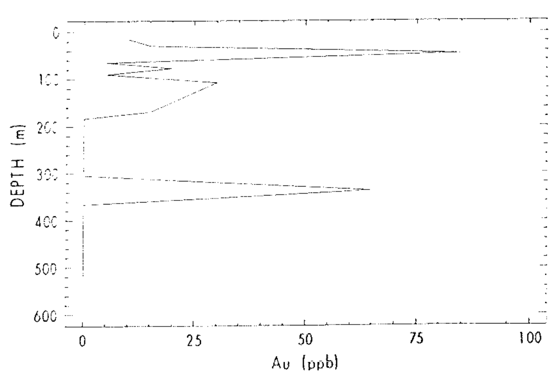

FIG. 3. Whole-rock gold content (ppb) versus depth (meters) for VC-2a drill core. Data from Musgrave et al. (1989).

from shallower fluids in VC-2a. This argues against significant sulfur contributions from biogenic sulfides or marine sulfates that may occur in lithologies beneath or peripheral to the volcanic section in the Sulphur Springs area. Thus, the sulfur isotope zoning from heavy cores to light rims in the pyrites from the 57.3-m level must instead reflect either changes in depositional conditions or fluid chemistry.

It is possible, in a sulfur-deficient system, to alter the sulfur isotope composition of aqueous H_2S through closed-system precipitation of sulfide minerals (e.g., Ohmoto, 1986) and such a phenomenon may have occurred, for example, during deposition of some of the vein sulfide minerals in the Salton Sea geothermal system (McKibben and Eldridge, 1989). Equilibrium closed-system precipitation of pyrite must move the $\delta^{34}S$ value of aqueous H_2S to lower values and this could account for some of the isotopic shift observed in the zoned crystals from the 57.3-m level in the Valles caldera as well. However, because of the mineralogic and fluid inclusion evidence for boiling in the shallow Valles caldera system, it is unlikely that closed-system precipitation effects caused the radical shifts in $\delta^{34}S$ observed in the zoned pyrites.

Increasing oxidation state can also lead to lower $\delta^{34}S$ values for H_2S (e.g., Ohmoto and Rye, 1979) and large negative shifts in pyrite isotopic conditions would result. It is also possible that a departure from equilibrium occurred and kinetic effects, leading to a rapid preferential oxidation of ^{34}S, dominated. Seven out of the ten crystals from the 57.3-m level show some effects of a process which caused the large isotopic shift and it is likely, therefore, that an overall oxidative event is responsible for the change.

A boiling event, with concomitant H_2 loss, would push the compositions of the remaining fluid to a more oxidized state (Drummond and Ohmoto, 1985). Thermodynamic calculations by Reed and Spycher (1985) indicate that H_2S should be progressively oxidized to SO_4 during boiling. This could allow rapid preferential oxidation of ^{34}S in H_2S and its incorporation into $^{34}SO_2$ or $^{34}SO_4$. A potential mechanism can be outlined as follows.

It has been shown experimentally that H_2 loss during boiling is kinetically faster than H_2S loss (Brown, 1989):

$$H_2S_{(aq)} \rightarrow H_2S_{(g)} \quad \text{(slow)} \qquad (3)$$

and

$$H_{2(aq)} \rightarrow H_{2(g)} \quad \text{(fast)}, \qquad (4)$$

probably reflecting the differences in dipole moments and sizes between the two gas species. Rapid loss of H_2 therefore may result in oxidation of aqueous H_2S during boiling:

$$H_2S_{(aq)} + 2H_2O \rightarrow SO_{2(g)} + 3H_{2(g)} \qquad (5)$$

or

$$H_2S_{(aq)} + 4H_2O \rightarrow SO_4^{-2} + 2H^+ + 4H_{2(g)}. \qquad (6)$$

Such oxidation would lead to preferential partitioning of ^{34}S into SO_2, SO_4^{-2}, or some other sulfur oxyanion (Ohmoto and Rye, 1979; Ohmoto and Lasaga, 1982):

$$H_2^{34}S_{(aq)} + 4H_2O \rightarrow {}^{34}SO_{4(aq)}^{-2} + 2H^+ + 4H_{2(g)}. \qquad (7)$$

Such an effect would leave progressively lighter H_2S behind in the liquid phase, to be incorporated into pyrite:

$$2H_2^{32}S_{(aq)} + Fe^{+2} \rightarrow Fe^{32}S_2 + H_{2(g)} + 2H^+. \qquad (8)$$

The overall result would be pyrite crystals that are isotopically zoned from heavy cores to light rims. The degree of zoning could be quite variable, depending on the exact point in time during boiling that crystal growth began and ended, the growth rate of pyrite, the temperature, and the rate of H_2S oxidation.

The viability of this proposed mechanism for producing isotopically zoned pyrite can be tested by applying the Rayleigh distillation equation (e.g., Valley, 1986):

$$\delta_{\text{final}} - \delta_{\text{final}} = 1{,}000(F^{(\alpha-1)} - 1), \qquad (9)$$

where F is the fraction of species removed and α is the fractionation factor upon removal. For an equilibrium fractionation of $\simeq$30 per mil between H_2S and SO_4 at 200°C (Ohmoto and Lasaga, 1982), the removal of H_2S via oxidation to SO_4 will yield residual aqueous H_2S that is depleted by 3 per mil at 10 percent removal, 9 per mil at 25 percent removal, and 21 per mil at 50 percent removal. Thus, isotopic shifts on the order of those observed for the zoned VC-2a pyrites can be produced easily by boiling-induced oxidation of aqueous H_2S.

It may be that a general link between radical sulfur isotope zonation and gold deposition exists in boiling systems. Gold, transported as an aqueous bisulfide complex, is easily precipitated from an oxidizing or boiling fluid (Reed and Spycher, 1985; Brown, 1986; Seward, 1989). The same combination of H_2 and H_2S loss that drives the isotopic zoning also drives the destabilization of Au bisulfide complexes and promotes gold deposition via reactions such as:

$$AuHS^0 + H^+ \rightarrow Au^+ + H_2S_{(g)} \qquad (10)$$

and

$$AuHS^0 + 4H_2O \rightarrow Au^+ + 4H_{2(g)} + SO_4^{-2} + H^+. \qquad (11)$$

If such a causative link exists, then levels where strong isotopic zonation occurs should coincide with levels where gold enrichment occurs. The shallow phyllic zone of VC-2a does contain elevated contents of Au (Fig. 3), with a maximum near the depths where we observed radical sulfur isotope zoning of pyrites.

Proposal of boiling as the main mechanism responsible for coupled isotopic zoning in pyrite and gold deposition is consistent with the general geology of the Valles caldera system and with the textures and phyllic mineral assemblages found in the VC-2a drill core (Hulen and Nielsen, 1988). Extremely wide ranges in homogenization temperatures of primary fluid inclusions in quartz and fluorite (Fig. 4) also support a boiling model for the mineralization.

While the sulfur isotope zonation, fluid inclusion evidence, alteration assemblages, and whole-rock Au enrichments comprise a consistent set of indicators of a paleoboiling zone near the 57.3-m level, the restriction of the zoned pyrites to this level requires some discussion. The fluid inclusion data of Gonzalez (1989; Fig. 4) and Sasada and Goff (1989) imply that

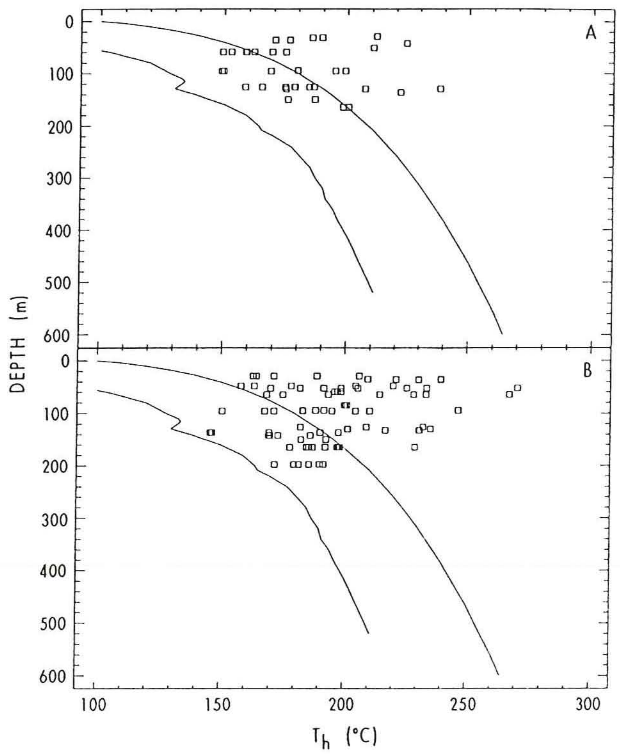

FIG. 4. Homogenization temperatures of primary (A) and secondary (B) fluid inclusions in vein quartz and fluorite versus depth (in m) in VC-2a drill core (modified from Gonzalez, 1989). Upper smooth curve is the boiling-point curve for a column of water having the composition of present-day VC-2a fluid; lower irregular curve is present-day measured downhole temperature.

boiling occurred throughout the phyllic zone and was not limited to the 57.3-m level. It is possible that our limited sampling (three depths) has simply missed isotopic evidence of boiling at other levels. Nonetheless, the strong isotopic heterogeneity correlates well with the maximum in Au values near the 51-m level (Fig. 3), suggesting that boiling was especially vigorous or long-lived near this level. The homogeneous pyrite deposited at the 30.5- and 129.6-m levels may have been deposited early from single-phase fluids, before the main boiling event. It is possible that the cores of the strongly zoned pyrites from the 57.3-m level were also deposited before boiling, with the lighter rims being precipitated during boiling.

Conclusions and Implications

Precious metals deposition, through boiling-induced destabilization of sulfide complexes, has been recorded by small-scale radical sulfur isotope zonation (up to 22‰ over 75 μm) in individual pyrite crystals from the shallow phyllic alteration zone of the Valles caldera. These isotopic signatures, which might have been missed in a study using conventional bulk isotopic analyses, have been readily discovered using an in situ microanalytical technique. Other SHRIMP sulfur isotope data from less pristine terranes, such as the greenschist-grade Rammelsberg deposit (Eldridge et al., 1988a) or the greenschist-amphibolite-grade Salton Sea metasediments (McKibben and Eldridge, 1989) suggest that such microscale isotopic heterogeneity may be preserved in spite of deposit metamorphism. Therefore, in deposits in which other evidence of an epithermal origin (such as acid alteration assemblages and fluid inclusions) might have been obliterated by subsequent processes, it might be feasible to identify paleoboiling horizons enriched in precious metals through examination of the sulfur isotope characteristics of sulfide crystals. Further research might include examination of the sulfur isotope compositions of pyrite crystals from suspected metamorphosed epithermal gold deposits in greenstone belts.

Acknowledgments

This research was supported by National Science Foundation grant EAR-88-15502 to M.A.M. Financial support for C.S.E. was provided by the Australian Research Council; the visiting fellowship granted by the Research School of Earth Sciences is also acknowledged. The authors are grateful to Fraser Goff, Jeff Hulen, Larry Maassen, and John Musgrave for valuable discussions and assistance in sample selection. Discussion of the results with W. C. Shanks III was greatly appreciated.

April 10, August 8, 1990

REFERENCES

Berger, B. R., and Bethke, P. M., eds., 1985, Geology and geochemistry of epithermal systems: Rev. Econ. Geology, v. 2, 298 p.

Brown, K. L., 1986, Gold deposition from geothermal discharges in New Zealand: ECON. GEOL., v. 81, p. 979-983.

——1989, Kinetics of gold precipitation from experimental hydrothermal sulfide solutions: ECON. GEOL. MON. 6, p. 320-327.

Charles, R. W., Buden, R. J. V., and Goff, F., 1986, An interpretation of the alteration assemblages at Sulphur Springs, Valles caldera, New Mexico: Jour. Geophys. Research, v. 91, no. B2, p. 1887-1898.

Drummond, S. E., and Ohmoto, H., 1985, Chemical evolution and mineral deposition in boiling hydrothermal systems: ECON. GEOL., v. 80, p. 126-147.

Eldridge, C. S., Compston, W., Williams, I. S., Walshe, J. L., and Both, R. A., 1987, In situ microanalysis for $^{34}S/^{34}S$ ratios using the ion microprobe SHRIMP: Internat. Jour. Mass Spectrometry Ion Processes, v. 76, p. 65-83.

Eldridge, C. S., Compston, W., Williams, I. S., Both, R. A., Walshe, J. L., and Ohmoto, H., 1988a, Sulfur isotope variability in sediment-hosted massive sulfide deposits as determined using the ion microprobe SHRIMP: I. An example from the Rammelsberg orebody: ECON. GEOL., v. 83, p. 443-449.

Eldridge, C. S., Williams, N., Compston, W., and Walshe, J. L., 1988b, SHRIMP ion microprobe investigation of the sulfur isotopic composition of the H.Y.C. Pb-Zn deposit, McArthur River, Australia [abs.]: Geol. Soc. America Abstracts with Programs, v. 20, p. 303.

Eldridge, C. S., Compston, W., Williams, I. S., and Walshe, J. L., 1989, Sulfur isotope analyses on the SHRIMP ion microprobe: U. S. Geol. Survey Bull. 1890, p. 163-174.

Goff, F., Nielson, D. L., Gardner, J. N., Hulen, J. B., Lysne, P., Shevenell, L., and Rowley, J. C., 1987, Scientific drilling at Sulphur Springs, Valles caldera, New Mexico—core hole VC-2a: Am. Geophys. Union Trans., v. 68, p. 649 and 661-662.

Gonzalez, C. M., 1989, Fluid inclusion study of the vein mineralization in the VC-2a corehole, Valles caldera, New Mexico: Unpub. M.S. thesis, Univ. California, Riverside, 107 p.

Hulen, J. B., and Gardner, J. N., 1989, Field geologic log for Continental Scientific Drilling Program corehole VC-2b, Valles caldera, New Mexico: Univ. Utah Research Inst. Earth Sci. Lab. Rept. ESL-89025-TR, 92 p.

Hulen, J. B., and Nielson, D. L., 1988, Clay mineralogy and zoning in CSDP corehole VC-2a: Further evidence for collapse of isotherms in the Valles caldera: Geothermal Resources Council Trans., v. 12, p. 291-298.

Hulen, J. B., Goff, F., Nielson, D. L., Gardner, J. N., and Charles, R., 1987, Molybdenum mineralization in an active geothermal system, Valles caldera, New Mexico: Geology, v. 15, p. 748-752.

McKibben, M. A., and Eldridge, C. S., 1989, Sulfur isotopic variations among minerals and aqueous species in the Salton Sea geothermal system: A SHRIMP ion microprobe and conventional study of active ore genesis in a sediment-hosted environment: Am. Jour. Sci., v. 289, p. 661-707.

Musgrave, J. A., Goff, F., Shevenell, L., Trujillo, P. E., Jr., Counce, D., Luedemann, G., Garcia, S., Dennis, B., Hulen, J. B., Janik, C., and Tomei, F. A., 1989, Selected data from Continental Scientific Drilling core holes VC-1 and VC-2a, Valles caldera, New Mexico: Los Alamos Natl. Lab. Rept. LA-11496-OBES, 71 p.

Ohmoto, H., 1986, Stable isotope geochemistry of ore deposits: Rev. Mineralogy, v. 16, p. 491-560.

Ohmoto, H., and Lasaga, A. C., 1982, Kinetics of reactions between aqueous sulfates and sulfides in hydrothermal systems: Geochim. et Cosmochim. Acta, v. 46, p. 1727-1746.

Ohmoto, H., and Rye, R. O., 1979, Isotopes of sulfur and carbon, *in* Barnes, H. L., ed., Geochemistry of hydrothermal ore deposits: New York, Wiley-Intersci., p. 509-567.

Plumlee, G. S., and Rye, R. O., 1987, Mineralization in the waning Creede epithermal system, and similar behavior in other systems [abs.]: Geol. Soc. America Abstracts with Programs, v. 19, p. 807.

Reed, M. H., and Spycher, N. F., 1985, Boiling, cooling, and oxidation in epithermal systems: A numerical modeling approach: Rev. Econ. Geology, v. 2, p. 249--272.

Sasada, M., and Goff, F. E., 1989, Fluid inclusions in minerals from the VC-2a core hole of CSDP at the Valles caldera, New Mexico [abs.]: Biennial Pan-American Conference on Research on Fluid Inclusions, 2nd, January 4-7, 1989, Blacksburg, VA, Program and Abstracts, p. 57.

Seward, T. E., 1989, The hydrothermal chemistry of gold and its implications for ore formation: Boiling and conductive cooling as examples: ECON. GEOL. MON. 6, p. 398-404.

Valley, J. W., 1986, Stable isotope geochemistry of metamorphic rocks: Rev. Mineralogy, v. 16, p. 445-490.